AUT Journal of Mathematics and Computing

AUT J. Math. Comput., 2(2) (2021) 153-163
DOI: 10.22060/ajmc.2021.20213.1059

On spectral data and tensor decompositions in Finslerian framework

Vladimir Balan*[a]

[a]*Department of Mathematics-Informatics, Faculty of Applied Sciences, University Politehnica, Bucharest, Romania*

ABSTRACT: The extensions of the Riemannian structure include the Finslerian one, which provided in recent years successful models in various fields like Biology, Physics, GTR, Monolayer Nanotechnology and Geometry of Big Data. The present article provides the necessary notions on tensor spectral data and on the HO-SVD and the Candecomp tensor decompositions, and further study several aspects related to the spectral theory of the main symmetric Finsler tensors, the fundamental and the Cartan tensor. In particular, are addressed two Finsler models used in Langmuir-Blodgett Nanotechnology and in Oncology. As well, the HO-SVD and Candecomp decompositions are exemplified for these models and metric extensions of the eigenproblem are proposed.

Review History:

Received:28 June 2021
Accepted:24 July 2021
Available Online:01 September 2021

Keywords:

Pseudo-Finsler structure
Symmetric tensors
Spectral data
Cartan tensor
HO-SVD decomposition
Candecomp approximation

AMS Subject Classification (2010):

65F30; 15A18; 15A69; 53B40; 53C60

(*Dedicated to Professor Zhongmin Shen for his warm friendship and research collaboration)*

1. Introduction

The attempt of extending the eigendata of linear operators in finite-dimensional vector spaces to symmetric covariant tensors in a natural way was a notable subject along recent years, providing different approaches [1, 2]. Related to this, it was shown that there exist also multiple ways to provide canonic Tucker type decompositions for tensors ([3]-[8]). On the other hand, remarkable symmetric tensors which occur in the Finslerian geometric models ([9]-[13]), which are relevant for the structure naturally admit relevant eigendata and Tucker decompositions ([14]-[16]). The works dedicated to their various applications (we mention [17]-[20]) are accompanied by the the strive to obtain optimal symbolic computational means (e.g., [21]-[27]).

The present work illustrates this multilinear algebraic approach for two pseudo-Finsler structures: one produced by the process of formation of the Langmuir-Blodgett monolayers from Nanotechnology [28, 29] and the second of Randers type, statistically associated to the Garner dynamical system from Oncology [30, 31]. Covariant extensions for the tensor eigenproblem are proposed and discussed, within the Riemannian and Finslerian frameworks.

*Corresponding author.
E-mail addresses: vladimir.balan@upb.ro

2. Tensorial extensions of the matrix eigenproblem

The attempt of naturally extending the eigenproblem for bilinear forms in finite-dimensional vector spaces to multi-index symmetric covariant tensors (N-way arrays) can be achieved in several ways [1, 2], as follows.

Let $T \in \mathcal{T}_m^0(\mathbb{R}^n)$ be a symmetric tensor field on the flat manifold $V = \mathbb{R}^n$.

Definition 2.1. *For $T \in \mathcal{T}_m^0(\mathbb{R}^n)$ a symmetric tensor field on the flat manifold $V = \mathbb{R}^n$.*
a) The scalar $\lambda \in \mathbb{R}$ and the vector $y \in \mathcal{T}_0^1(\mathbb{R}^n) \equiv \mathbb{R}^n$ are respectively called $Z-$eigenvalue *($\lambda \in \sigma_Z(T)$), and the* associated $Z-$eigenvector *to λ, if they satisfy the system of $n+1$ equations:*

$$T \circ^{m-1} y = \lambda y; \quad g(y, y) = 1,$$

where $T \circ^{m-1} y = T_{k,i_2,\dots,i_m} y^{i_2} \dots y^{i_m} \cdot dx^k$. Moreover, for $\lambda \in \mathbb{C}$ and $y \in \mathbb{C}^n$ these are respectively called $E-$eigenvalue *and* $E-$eigenvector.

b) The scalar $\lambda \in \mathbb{R}$ and the vector $y \in \mathcal{T}_0^1(\mathbb{R}^n) \equiv \mathbb{R}^n$ are respectively called $H-$eigenvalue *($\lambda \in \sigma_H(T)$), and the* associated $Z-$eigenvector *to λ, if they satisfy the polynomial homogeneous of order $m-1$ system of n equations:*

$$(T \circ^{m-1} y)_k = \lambda (y^k)^{m-1}, \ \ k \in \overline{1, n}.$$

Moreover, for $\lambda \in \mathbb{C}$ and $y \in \mathbb{C}^n$ these are respectively called $N-$eigenvalue *and* $N-$eigenvector.

It was shown that $\sigma_Z(T) \neq \emptyset$ and $\sigma_E(T) \neq \emptyset$ for even-order symmetric tensors. As well, it was proved that the following concept of $B-$eigenvalue/eigenvector embraces both the $H-$ and $N-$cases of eigendata and, the $Z-$ and $E-$ones (in the even-order case).

Definition 2.2. *For two given $m-$order $n-$dimensional symmetric tensors T, B, we call $B-$eigenvalue and correspondingly $B-$eigenvector the couple $(\lambda, y) \in K \times K^n$ ($K \in \{\mathbb{R}, \mathbb{C}\}$) which satisfies the conditions:*

$$\sum_{i_2,\dots,i_m=1}^{n} (T_{ki_2\dots i_m} - \lambda B_{ki_2\dots i_m}) y_{i_2} \dots y_{i_m} = 0, \forall k \in \overline{1, n}. \tag{2.1}$$

Then the following result holds true [1, 2]:

Proposition 2.3. *a) The $Z-$ and $E-$eigenvalues are obtained as particular solutions of* (2.1)*, assuming m even, for:*

$$B_{i_1\dots i_m} = \delta_{i_1 i_2} \dots \delta_{i_{m-1} i_m}.$$

b) The $H-$ and $N-$ eigenvalues are obtained as particular solutions of (2.1)*, for*

$$B_{i_1\dots i_m} = \delta_{i_1\dots i_m} = \begin{cases} 1, & \text{for } i_1 = \dots = i_m, \\ 0, & \text{otherwise.} \end{cases}$$

The Candecomp polyadic decomposition.
For an arbitrary tensor $T \in \mathbb{R}^{I_1 \times I_2 \times \dots I_N}$, the general Candecomp (*Parafac*) decomposition has the form [3, 4]:

$$T = \sum_{r=1}^{R} \lambda_r \mathbf{v}_r^{(1)} \otimes \dots \otimes \mathbf{v}_r^{(N)},$$

where $B^{(s)} = [\mathbf{v}_1^{(s)}, \dots, \mathbf{v}_R^{(s)}] \in \mathcal{M}_{I_r \times R}(\mathbb{R})$, $s \in \overline{1, R}$ are the modal matrices, $\lambda_r \in \mathbb{R}$ ($r \in \overline{1, R}$) are scalars and $R \in \overline{0, N}$ is the *the rank* of the tensor [3, 4].

The best rank-one approximation of $T \in \mathcal{T}_m^0(\mathbb{R}^n)$, is the homogeneous polynomial $y-$ dependent tensor $A = \lambda \otimes^m \mathbf{y}^*$, which is global minimizer for the distance $||T - \lambda \otimes^m \mathbf{y}||_F$ for $\lambda \in \mathbb{R}, ||\mathbf{y}||_2 = 1$, where $|| \cdot ||_F$ is the Frobenius norm, and where $\otimes^m \mathbf{y}^*$ is be regarded as an $m-$th order $n-$dimensional degenerate tensor of rank 1, with the components $y_{i_1} \cdot \dots \cdot y_{i_m}$ [1, 2]. An important result which show that this approximate is an efficient estimate for T in applications, is the following:

Theorem 2.4. *Consider $T \in \mathcal{T}_m^0(\mathbb{R}^n)$. Then:*
a) For $\lambda \in \sigma_Z(T)$ and y its associated $Z-$eigenvector, we have $\lambda = Ty^m$ and

$$||T - \lambda \otimes^m \mathbf{y}||_F^2 = ||T||_F^2 - \lambda^2 \geq 0.$$

b) The best rank one approximation of T is provided by $A = \lambda \otimes^m \mathbf{y}$, where $\lambda = argmax|\sigma_Z(T)|$ and y is one of its eigenvectors.

As well, it is known that the best rank-one approximation of T is the solution of the variational equivalent to the dual problem of maximizing

$$f(y) = \Sigma_{i_1,\ldots,i_m=\overline{1,n}}\ T_{i_1\ldots i_m} y_{i_1}\ldots y_{i_m} = \langle T, \otimes^m y^*\rangle, \ \text{ for } ||y||_2 = 1,$$

equivalent to the maximization of the Rayleigh quotient

$$q(y) = \frac{\langle T, \otimes^m y^*\rangle^2}{\langle y, y\rangle^m} = \frac{f^2(y)}{||y||_2^{2m}}.$$

An important ingredient in constructing the solution to this problem is the $H-$spectral data (for $n > 2$), while the case of $n = 2$ reduces to the classic matrix spectral framework.

3. Finsler and pseudo-Finsler structures

We shall further consider the Finslerian framework, which naturally extends the Riemannian one.

Definition 3.1. *A real Finsler structure: a couple (M, F), such that:*
*M is a real n-dimensional C^∞ manifold; $F : TM \to [0, \infty)$ is a mapping (*Finsler fundamental function*), which satisfies:*

1. *F smooth on the slit tangent space $T_0M = \{(x, y)|x \in M, y \in T_xM, y \neq 0\}$ continuous on the null section;*
2. *F positive 1-homogeneous in y, i.e., $F(x, \lambda y) = \lambda F(x, y), \forall\lambda > 0$;*
3. *F defines the smooth maps $g_{ij} : TM \setminus \{0\} \to \mathbb{R}$, $i, j \in \overline{1, n}$ components of the metric Finsler tensor field $g = g_{ij}dx^i \otimes dx^j$, which form a symmetric positive definite matrix, $(g_{ij})_{i,j\in\overline{1,n}}$, $g_{ij} = \frac{1}{2}\frac{\partial^2 F^2}{\partial y^i \partial y^j}$.*

We shall also consider the pseudo-Finslerian extensions of this framework, in which F lacks the non-negativity condition, is only positive-homogeneous, and g is only non-degenerate.

Examples.

• In medical image analysis (more specific, in Diffusion Tensor Imaging DTI), the Riemannian-type diffusion norm

$$F = \sqrt{y^t D^{-1} y}, \ \ \forall y \in T_x\mathbb{R}^3,$$

(D being a 3×3 real matrix) was extended to the Finslerian ($HARDI$) model based on the spherical tensor [32] $D = \{D_{i_1\ldots i_6}\}$, which builds the Finsler 6−th root norm

$$F(x, y) = (D_{i_1\ldots y_6} y^{i_1}\ldots y^{i_6})^{1/6}, \ \ \forall y \in T_x\mathbb{R}^6;$$

• The m-th root Grobner-type Finsler pseudo-norms [33], including Berwald-Moor, Chernov and Bogoslovski [14, 15, 16];
• Kropina $\frac{\alpha^2}{\beta}$, Matsumoto $\frac{\alpha^2}{\alpha-\beta}$, and Randers $\alpha + \beta$ ($||\beta||_\alpha < 1$);
• The Antonelli $m-$th root conformal-locally Minkowski norm [34], where $\sigma = \alpha_i x^i$, $\alpha_i \in \mathbb{R}_+, i = \overline{1, n}$:

$$F(x, y) = e^{\sigma(x)} \sqrt[m]{\sum_{k=1}^{n} (y^k)^m},$$

• The Roxbourgh and Reza-Tavakol relativistic EPS-axioms satisfying Finsler norms (1992), including the pseudo-norm modeling the light propagation ($\varepsilon \to 0$ leads to the classic locally Minkowski case) in $\mathbb{R}^4$:

$$F(x, y) = \left((y^1)^2 - \frac{[(y^2)^2 + (y^3)^2 + (y^4)^2]^3}{[\varepsilon(y^1)^2 + (y^2)^2 + (y^3)^2 + (y^4)^2]^2}\right)^{1/2}.$$

3.1. Finslerian main symmetric tensors

Consider an $n-$dimensional pseudo-Finsler space (M, F). The main symmetric tensors of this structure are: the fundamental metric tensor g and the Cartan tensor C, having the components:

$$g_{ij} = \frac{1}{2}\frac{\partial^2 F^2}{\partial y^i \partial y^j}, \qquad C_{ijk} = \frac{1}{4}\frac{\partial^3 F^2}{\partial y^i \partial y^j \partial y^k}, \quad i, j, k \in \overline{1, n},$$

which have the following notable properties:

- the transvection property: $C_{ijk}(x,y)y^k = 0$; $g_{ij}(x,y)y^j = F\frac{\partial F}{\partial y^i}$;
- a Lagrange space (M, L) [12] becomes Finslerian iff C_{ijk} is completely symmetric and satisfyes the transvection property; in such a case, (M, F) with $L = F^2$ is a Finsler sructure;
- a Finsler space (M, F) becomes Riemannian (pseudo-Finsler $\rightsquigarrow$ pseudo-Riemannian) iff $C_{ijk} \equiv 0$; in such a case, we have the structure (M, g), with $g = \frac{1}{2}Hess_y(F^2)$ being $y-$independent.

Regarding *the Candecomp decomposition*, we have the following straightforward results

Proposition 3.2. *a) For* the (0,2) Finslerian metric tensor $T = g$ *considered at a fixed flagpole, the Candecomp decomposition becomes the adjusted SVD decomposition of $[g]$, directly inferred from the diagonalization via an orthonormal basis. The squares of the singular values are exactly the eigenvalues of the $k-$modes (de Lathauwer or Kiers).*
b) For the $(0, 3)$ Cartan tensor $T = \mathcal{C}$, *the Candecomp decomposition has the form:*

$$T = \sum_{r=1}^{R} \lambda_r \mathbf{a}_r \otimes \mathbf{b}_r \otimes \mathbf{c}_r,$$

with

$$A = [\mathbf{a}_1, \ldots, \mathbf{a}_N],\ B = [\mathbf{b}_1, \ldots, \mathbf{b}_N],\ C = [\mathbf{c}_1, \ldots, \mathbf{c}_N],$$

and $\lambda \in \mathbb{R}$, $r \in \overline{1,R}$, where R is the rank of T [3, 4]. The sum in b) can be truncated to the term corresponding to the $\lambda_* \in \sigma_Z$ which has maximal absolute value and $\mathbf{y}$ its corresponding $Z-$eigenvector, one gets the Candecomp approximation

$$T \approx \lambda_* \otimes^N \mathbf{y} = \lambda_* \mathbf{y} \otimes \mathbf{y} \otimes \mathbf{y}.$$

3.2. Spectral data

Consider a (pseudo-)Finsler space (M, F), and a given flag (x, y_*), which fixes the components of the Finsler tensor fields. In particular, for the metric and the Cartan tensors, we have the spectral $Z-$ and $E-$equations for the metric tensor of the space of the form

$$g_{ij}f^j = \lambda f^i,\ i \in \overline{1,n}, \quad \text{and} \quad C_{ijk}f^jf^k = \lambda f^i,\ i \in \overline{1,n}, \qquad \text{with } ||f||_2 = 1.$$

Let $T = T = (x,y)_{i_1 \ldots i_m} dx^{i_1} \otimes \ldots \otimes dx^{i_m} \in T^0_m(M)$ be an m-covariant symmetric homogeneous Finsler tensor with fixed flag (x, y). Denote by h_tT the tensor with homothetic flag $(h_tT)(x, y) = T(x, ty)$. Then, regarding to the behavior of spectra w.r.t. the flag homothety, and of eigenvalues under symmetry, we have:

Theorem 3.3. *a) For the metric tensor g, for all cases $Z/E/H/N$,*

$$\sigma(h_t g) = \sigma(g), \ \ \forall t \in D;$$

b) For the Cartan tensor C, for all cases $Z/E/H/N$,

$$\sigma(h_t C) = h_{1/t} \cdot \sigma(C), \ \ \forall t \in D,$$

where $D = \begin{cases} \mathbb{R}^* & \textit{for } F \textit{ homogeneous} \\ \mathbb{R}^*_+, & \textit{for } F \textit{ positive homogeneous.} \end{cases}$

We shall further provide an analysis for two Finsler structures, which appear in modeling the behavior of Langmuir monolayers under pressure; another, corresponding to the expectance in the evolution of an oncologic process after significant changes in the parameters.

4. The Langmuir-Finsler spectral data

Finsler geometry provides relevant geometric objects for the Physics of monolayers (e.g., [28, 29]). Far from the equilibrium state of a compressed monolayer there appears a phase foliation at which an interface boundary consists of domains of subphase surface, the Langmuir-Blodgett monolayer, and the Langmuir monolayer. We represent in Fig.1(a) the Langmuir monolayer and the double charged layer during the compression process. The three-dimensional globe conformation of the hydrophobic tails on the subphase surface is represented in Fig 1(b).

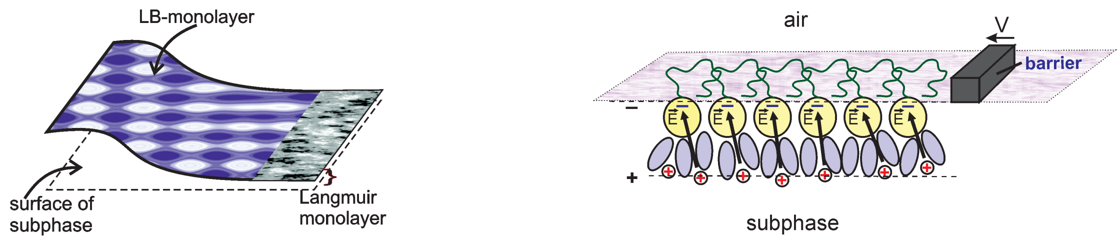

(a) The Langmuir-Blodgett monolayer formation (b) The subphase space.

Figure 1: First-order phase transition in Langmuir-Blodgett monolayers.

Under certain conditions, the behavior of the interface boundary of the monolayer is governed by the Finsler norm:

$$F^2 = A\frac{\dot{\xi}^3}{\dot{r}} + B\dot{\xi}^2 - C\frac{(\dot{r}^2 + r^2\dot{\phi}^2)}{2c^2},$$

where the parameters A, B, C are given by:

$$\begin{aligned} A &= p\,|V|\,r^5 e^{\frac{2|V|t}{r}}, \\ B &= mc^2 - p\left(\left(-\tfrac{4}{3}r^5 + \tfrac{16}{15}(|V|t)r^4 + \tfrac{1}{30}(|V|t)^2r^3 + \tfrac{1}{45}(|V|t)^3r^2 \right.\right. \\ &\quad \left.\left. + \tfrac{1}{45}(|V|t)^4r + \tfrac{2}{45}(|V|t)^5\right) e^{\frac{2|V|t}{r}} - \tfrac{4}{45}\tfrac{(|V|t)^6}{r}\mathrm{Ei}\left[\tfrac{2|V|t}{r}\right]\right), \\ C &= mc^2, \end{aligned}$$

where V is the compression speed, $\mathrm{Ei}\left[\frac{2|V|t}{r}\right]$ is the exponential integral, m is the molecular mass and c is he speed of light. Also, r and ϕ are the first two components of the cylindric orthogonal coordinate system (r, ϕ, z), in which the spherically-symmetric monolayer is displaced in the plane xy $(z = 0)$ and the center is located at the origin of coordinates. As admissible experimental values for the parameters we have:

$$\begin{aligned} &p \in \{1, 10\}, \quad V \in \{0, 10^{-15}, 10^{-5}, 10^{-3}, 0.05, 1, 10, 500\}, \quad \rho_0 = 0, \\ &q \in \{-0.1, 0, 0.1, 0.29\}, \quad R_0 = 0.36, \quad \varepsilon = 81, \quad \varepsilon_0 = 0.885 \cdot 10^{-11}, \\ &m = 47 \cdot 10^{-26}, \quad c = 3 \cdot 10^8, \quad t_0 = 0.01, \quad v = 0.05 \text{ and } r_0 \in [0, 0.36]. \end{aligned}$$

Regarding the spectra of the Blodgett-Finsler pseudo-metric and of the Cartan tensor, we have the following

Theorem 4.1. *a) For Z/E with m even, if $y \in S_\lambda$ $(\lambda \in \sigma)$, then $-y \in S_\lambda$;*

b) For Z/E with m odd, if $y \in S_\lambda$ $(\lambda \in \sigma)$, then $-\lambda \in \sigma$ and $-y \in S_{-\lambda}$;

c) For H/N, if $y \in S_\lambda$ $(\lambda \in \sigma)$, then $\forall t \in \mathbb{K}$, $ty \in S_\lambda$, where $\mathbb{K} \in \{\mathbb{R}, \mathbb{C}\}$, respectively.

The metric tensor of the LF structure has the attached matrix:

$$[g] = \begin{pmatrix} 3A\frac{y^1}{y^2} + B & -\frac{3}{2}A\frac{(y^1)^2}{(y^2)^2} & 0 \\ -\frac{3}{2}A\frac{(y^1)^2}{(y^2)^2} & A\frac{(y^1)^3}{(y^2)^3} - \frac{1}{2}C & 0 \\ 0 & 0 & -\frac{1}{2}C(x^2)^2 \end{pmatrix},$$

with $(x^1, x^2, x^3) = (\xi, r, \phi)$ and $(y^1, y^2, y^3) = (\dot{\xi}, \dot{r}, \dot{\phi})$.

As for the Candecomp and HO-SVD decompositions, we have the following results:

We shall further assume that the supporting element $(x, y_*) \in \widetilde{TM}$ is fixed.

I. The metric tensor.

We note that the matrix $[g]$ is symmetric, and for experimentally admissible values of A, B, C, it is non-definite, non-degenerate, of signature $(+, +, -)$. Since the metric tensor g is of second order, the CP and $HO - SVD$ decompositions coincide, and are practically provided by the usual SVD decomposition. The CP approximation is given by the eigendata of the maximal positive eigenvalue of $[g]$. The matrix $[g]$ admits the real eigenvalues

$$\sigma([g]) = \left\{ \lambda_1 = \frac{L + \sqrt{R}}{4(y^2)^3},\ \lambda_2 = \frac{L - \sqrt{R}}{4(y^2)^3},\ \lambda_3 = -\frac{1}{2}C(x^2)^2 \right\},$$

where

$$\begin{aligned} L = \;& -C(y^2)^3 + 2A(y^1)^3 + 6(y^2)^2 A(y^1) + 2(y^2)^3 B \\ R = \;& C^2(y^2)^6 - 4A(y^1)^3 C(y^2)^3 + 12(y^2)^5 A(y^1) C + 4(y^2)^6 BC + \\ & +4A^2(y^1)^6 + 12(y^2)^2 A^2(y^1)^4 - 8(y^2)^3 BA(y^1)^3 + \\ & +36(y^2)^4 A^2(y^1)^2 + 24(y^2)^5 A(y^1) B + 4(y^2)^6 B^2, \end{aligned}$$

and three associated generating column eigenvectors

$$\Theta = [v_1; v_2; v_3] = \begin{pmatrix} \frac{3A(y^1)^2}{-2(y^2)\left(\frac{L+\sqrt{R}}{4(y^2)^2}+3A(y^1)+B(y^2)\right)} & \frac{3A(y^1)^2}{-2(y^2)\left(\frac{L-\sqrt{R}}{4(y^2)^2}+3A(y^1)+B(y^2)\right)} & 0 \\ 1 & 1 & 0 \\ 0 & 0 & 1 \end{pmatrix}$$

Then, for $D = \mathrm{diag}(\lambda_1, \lambda_2, \lambda_3)$, $E = [\frac{v_1}{||v_1||}, \frac{v_2}{||v_2||}, \frac{v_3}{||v_3||}] = [w_1, w_2, w_3]$, we have $D = E^t[g]E$, and infer the Candecomp decomposition by diagonalization relative to the orthonormal basis:

$$[g] = EDE^t = \sum_{i=\overline{1,3}} \lambda_i w_i \cdot w_i^t.$$

By denoting the eigenvalue of maximal absolute value by λ_* and the associated unit eigenvector by w_*, the best rank-one approximation of $[g]$ is $[g] \sim A = \lambda_* w_* \cdot w_*^t$.

With the same notations, the *HO-SVD* of $[g]$ is practically *SVD*, given by

$$\begin{aligned} [g] = \;& [\mathrm{sign}(\lambda_1) w_1, \mathrm{sign}(\lambda_2) w_2, \mathrm{sign}(\lambda_3) w_3] \cdot \mathrm{diag}(|\lambda_1|, |\lambda_2|, |\lambda_3|) \cdot [w_1, w_2, w_3]^t \\ = & \sum_{i=\overline{1,3}} |\lambda_i| \cdot (\mathrm{sign}(\lambda_i) w_i) \cdot w_i^t. \end{aligned}$$

II. The Cartan tensor. The Cartan tensor, considered at the fixed supporting element $(x, y_*) \in \widetilde{TM}$

$$C = C_{ijk}(x, y_*) dx^i \otimes dx^j \otimes dx^k, \quad C_{ijk}(x, y) = \frac{1}{4} \frac{\partial^3 F^2}{\partial y^i \partial y^j \partial y^k},$$

is a third-order covariant tensor, with its first-index slices given by

$$C = \{ ((C_{1ij} = \gamma \cdot M, \; C_{2ij} = \nu \cdot M, \; C_{3ij} = O_{3\times 3})) \}, \quad \text{where } \gamma = \frac{3A}{\beta^3}, \quad \nu = -\frac{\alpha}{\beta}\gamma,$$

where $y_* = (\alpha, \beta, \gamma)$ is the flag vector of the supporting element, and $M = \begin{pmatrix} \beta^2 & -\alpha\beta & 0 \\ -\alpha\beta & \alpha^2 & 0 \\ 0 & 0 & 0 \end{pmatrix}$. We note that C has only 8 nontrivial coefficients.

The Z/E-eigendata of the Cartan tensor are given by the eigensystem:

$$C_{kij} z^i z^j = \lambda z^k, \;\; k \in \overline{1,3}, \quad \sum_{i=\overline{1,3}} (z^i)^2 = 1,$$

which lead to

$$S_{\lambda_1=0} = \left\{ \frac{1}{\sqrt{\alpha^2+\beta^2+t^2}} (\alpha, \beta, t) \middle| \, t \in \mathbb{R} \right\}, \quad S_{\lambda_2 = \frac{9A^2}{\beta^8 \sqrt{\alpha^4+\beta^4}}} = \left\{ \frac{\pm 1}{\sqrt{\alpha^4+\beta^4}} (\beta^2, \alpha^2, 0) \right\}.$$

and which infer the twofold Candecomp approximation:

$$C \sim A = \lambda_2 \cdot v_\pm \otimes v_\pm \otimes v_\pm, \;\; v_\pm \in S_{\lambda_2}.$$

As well, the *H/N-homogeneous* eigensystem

$$C_{kij} z^i z^j = \lambda (z^k)^2, \;\; k \in \overline{1,3}$$

provides the H/N-eigendata:

$$S_{\lambda_1=0} = \left\{ \frac{1}{\sqrt{\alpha^2+\beta^2+t^2}} (\alpha, \beta, t) \middle| \, t \in \mathbb{R} \right\}, \quad S_{\lambda_2 = \frac{9A^2(\beta^2-\alpha^2)^2}{\beta^8}} = \left\{ \pm \left(\frac{\beta}{\sqrt{\alpha^2+\beta^2}}, \frac{-\alpha}{\sqrt{\alpha^2+\beta^2}}, 0 \right) \right\}.$$

For the *HO-SVD* decomposition of the Cartan tensor C, the de Lathauwer or Kiers matrix [3] matricization *unfolding* provides the three $k-$modes $\{M_1, M_2, M_3\} \in \mathcal{M}_{3\times 9}(\mathbb{R})$, which produce the singular values as square roots of the eigenvalues of $N_i = M_i \cdot M_i^t,\ i \in \overline{1,3}$:

$$\sigma_{sing} = \{\lambda_{sing_*} = (\alpha^2+\beta^2)\sqrt{\gamma^2+\nu^2},\ \ 0, 0\ \ \},$$

and the corresponding HO-SVD orthogonal matrices

$$U = \begin{pmatrix} \gamma/\sqrt{\gamma^2+\nu^2} & -\nu/\sqrt{\gamma^2+\nu^2} & 0 \\ \nu/\sqrt{\gamma^2+\nu^2} & \gamma/\sqrt{\gamma^2+\nu^2} & 0 \\ 0 & 0 & 1 \end{pmatrix}, \quad V = \begin{pmatrix} -\beta/\sqrt{\alpha^2+\beta^2} & \alpha/\sqrt{\alpha^2+\beta^2} & 0 \\ \alpha/\sqrt{\alpha^2+\beta^2} & \beta/\sqrt{\alpha^2+\beta^2} & 0 \\ 0 & 0 & 1 \end{pmatrix} = W,$$

with the columns conveniently permuted to satisfy the generalized core tensor slice orthonormality condition for the core tensor S; these lead to the HO-SVD for the Cartan tensor C:

$$C_{ijk}U_p^iV_q^jW_r^k = S_{pqr} \Leftrightarrow C_{ijk} = S_{pqr}(U^t)_i^p(V^t)_j^q(W^t)_k^r,$$

with the core tensor S almost zero (except $S_{111} = S_{222} = \lambda_{sing_*}$).

5. The Garner-Randers spectral data

In Oncology, the Garner-Randers structure provides information on the ratio of malignant/quiescent cells assuming that certain treatment conditions are fulfilled. The Garner model is described by the dynamical system

$$\begin{cases} \frac{d}{dt}x^1 = x^1 - x^1(x^1-x^2) + \frac{hx^1x^2}{1+k(x^1)^2} \\ \frac{d}{dt}x^2 = -rx^2 + ax^1(x^1-x^2) - \frac{hx^1x^2}{1+k(x^1)^2}, \end{cases}$$

- x, proliferating (*malignant*) cells, scaled;
- y, quiescent cells, scaled;
- a, which measures the relative nutrient uptake by resting vs. proliferating cancerous cells;
- $r = d/b$, the ratio between the death rate of quiescent cells and the birth rate of proliferating cells;
- h, growth factor that preferentially shifts cells from quiescent to proliferating state; it is inversely proportional to a;
- k, mild moderating factor.

For the experimental data

$$a = 1.998958904,\ r = 0.03,\ h = 1.236,\ k = 0.236,$$

and with *LSM* accuracy, we obtain the statistically fit local Garner-Randers Finsler estimate [30, 31]:

$$F(x,y) = \alpha+\beta \equiv \sqrt{g_{ij}(x)y^iy^j} + b_i(x)y^i = \sqrt{(y^1)^2+(y^2)^2} + 0.63y^1 - 0.27y^2,$$

where α is a y_*-dependent Riemannian norm and β is its linear deformation. The main multilinear symmetric tensors on $\{(x, y_*)\} \times T_x(M)$ are:

- the fundamental metric tensor $g(y_*) \equiv (g_{ij}(y))_{2x2}|_{y=y_*}$

$$g_{11} = \frac{1.26(y^1)^3+1.89y^1(y^2)^2+1.397\sqrt{(y^1)^2+(y^2)^2}((y^1)^2+(y^2)^2)-0.27(y^2)^3}{((y^1)^2+(y^2)^2)^{3/2}}$$

$$g_{12} = \frac{0.63(y^2)^3-0.27(y^1)^3-0.17\sqrt{(y^1)^2+(y^2)^2}((y^1)^2+(y^2)^2)}{((y^1)^2+(y^2)^2)^{3/2}}$$

$$g_{22} = \frac{0.63(y^1)^3-0.81(y^1)^2y^1+1.073\sqrt{(y^1)^2+(y^2)^2}((y^1)^2+(y^2)^2)-0.54(y^2)^3}{((y^1)^2+(y^2)^2)^{3/2}}$$

- the Cartan tensor $C(y_*) \equiv (C_{ijk}(y_*))_{2x2x2}|_{y=y_*}$

$$C_{111} = \frac{0.135(y^2)^3(7y^2+3y^1)}{((y^1)^2+(y^2)^2)^{-5/2}}, \quad C_{112} = \frac{-0.135(y^2)^2y^1(7y^2+3y^1)}{((y^1)^2+(y^2)^2)^{-5/2}},$$

$$C_{122} = \frac{0.135(y^1)^2y^2(7y^2+3y^1)}{((y^1)^2+(y^2)^2)^{-5/2}}, \quad C_{222} = \frac{-0.135(y^1)^3(7y^2+3y^1)}{((y^1)^2+(y^2)^2)^{-5/2}}.$$

The Z-eigendata are (λ, z) where $z = (z^1, z^2)$ are provided by the following eigensystems:

- for the Euclidean/Kronecker spectral framework with $\sigma_{Z_\delta} = \{0, 0, \lambda_d, -\lambda_d\}$,

$$C_{ijk}\delta^{ia}z^j z^k = \lambda z^a, \quad a = 1, 2; \qquad g_{ij}z^i z^j = 1;$$

- For the extended fixed-flag metric framework with $\sigma_{Z_g} = \{0, 0, \lambda_g, -\lambda_g\}$,

$$C_{ijk}z^j z^k = \lambda g_{ia}z^a, \quad i = 1, 2. \quad g_{jk}z^j z^k = 1.$$

We note that 0 is a Z-eigenvalue with multiplicity 2, and that (λ, z) is an eigenpair iff $(-\lambda, -z)$ is an eigenpair as well. In order to provide relevant numeric solutions for the Cartan Z-eigenproblem, we fix the following eigendata details: the flagpoles are unit subsequent vectors lying on the indicatrix (displaced via "indicatrix harmonics"):

$$(y^1, y^2) = \frac{1}{\|(\cos\theta, \sin\theta)\|_g} \cdot (\cos\theta, \sin\theta),$$

for $N = 64$, $\theta = h\frac{2\pi}{N}$, $h = \overline{1, N}$. The Garner-Randers indicatrix is harmonically digitized by using g-unit flagpoles - see Fig. 2(a). The Z-eigensystem can be tracted by Maple PolynomialSolve or Matlab providing the eigenpairs with h-dependent accuracy:

$$(\lambda(y^1, y^2) \rightsquigarrow z = z^1(y^1, y^2), z^2(y^1, y^2)),$$

and the Z_δ-eigendata for the nontrivial flag-dependent eigenvalues are represented in Fig. 2(b).

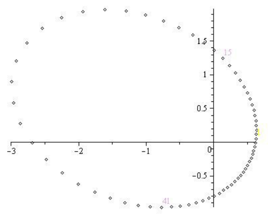

(a) Harmonic sampling of the indicatrix

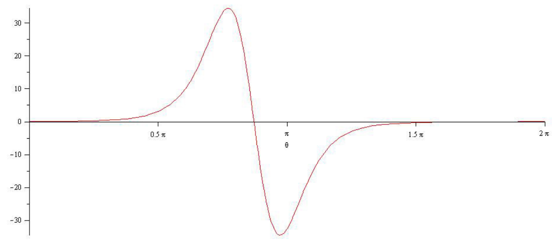

(b) Z_δ-eigendata

Figure 2: Harmonic sampling of the indicatrix and Z_δ-eigendata

As well, the Z_g-eigendata for the nontrivial eigenvalues can be depicted as follows:

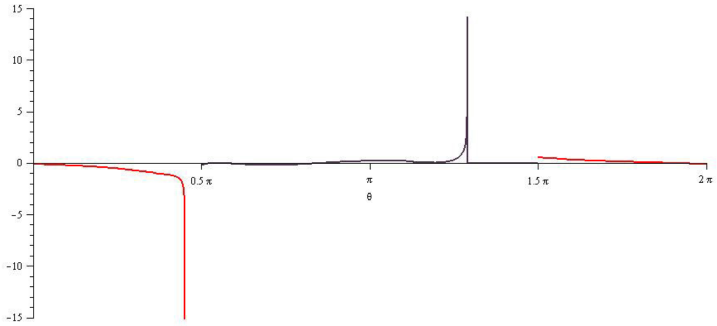

Figure 3: In this case, there exist non-real solutions of the Z-eigenproblem. For a whole flagpole subdomain, the eigenvalues are purely imaginary; their modules are plotted by the dark curve.

6. The Finslerian metric extension

We shall further describe the case of constructing the coordinate-independent formulation of the extended eigenproblem. For the beginning, the particular Riemannian Z/E frameworks can be developed as follows. Let $A = (A_{i\,i_2 \cdots i_m})$ be an m-th order tensor, covariant and symmetric, and let g be a Riemannian metric on M.

	Z/E	H/N
	$\begin{cases} A_{ii_2\cdots i_m}v^{i_2}\cdots v^{i_m}=\lambda v^i \\ v^T v=1 \end{cases}$	$A_{ii_2\cdots i_m}v^{i_2}\cdots v^{i_m}=\lambda (v^i)^{m-1}$
wrt δ	$\begin{cases} A_{ii_2\cdots i_m}\delta^{ia}v^{i_2}\cdots v^{i_m}=\lambda v^a \\ \lVert v\rVert_g=1 \end{cases}$	$A_{ii_2\cdots i_m}\delta^{ia}v^{i_2}\cdots v^{i_m}=\lambda (v^a)^{m-1}$
wrt g	$\begin{cases} A_{ii_2\cdots i_m}g^{ia}v^{i_2}\cdots v^{i_m}=\lambda v^a \\ \lVert v\rVert_g=\ell,\ \ \ell\in\mathbb{R} \end{cases}$	$A_{ii_2\cdots i_m}g^{ia}v^{i_2}\cdots v^{i_m}=\lambda (v^a)^{m-1}$

We note that the advantage of the g-left extension is its being coordinate-free, while the right extension exhibits homogeneity. As well, for $m=2$, the extensions reduce to the classical matrix eigensystem.

As for the proper Finslerian invariant case, we have the following results:

Theorem 6.1. *a) For $T\in\Gamma(\widetilde{TM}\times_M T^1_{2k})$ $(k\geq 1)$, the $Z-$spectral equation admits the following invariant extension:*

$$\iota^{2k}_{\mathcal{C}}T=\lambda\mathcal{C}\cdot(\iota^2_{\mathcal{C}}g)^k,$$

where $\mathcal{C}=y^i\frac{\partial}{\partial y^i}$ is the Liouville vector field.

b) For $T\in\Gamma(\widetilde{TM}\times_M T^1_{2k-1})$ $(k\geq 1)$, the $Z-$spectral equation admits the following invariant extension:

$$\iota^{2k-1}_{\mathcal{C}}T=\lambda\mathcal{C}.$$

Corollary 6.2. *For $T\in\Gamma(\widetilde{TM}\times_M T^0_{2k+1})$ $(k\geq 1)$, the $Z-$spectral equation admits the following invariant extension:*

$$\iota^{2k}_{\mathcal{C}}T=\lambda\iota_{\mathcal{C}}g\cdot(\iota^2_{\mathcal{C}}g)^k.$$

In particular, for the Cartan tensor, in the metric-extended σ_g case, we infer the following

Corollary 6.3. *a) Let $T=C\in\Gamma(\widetilde{TM}\times_M T^0_3)$, be the Cartan tensor considered at an arbitrary fixed flagpole $(x,y_*)\in M\times T_xM$. Then the local extended $Z-$spectral equation becomes*

$$C_{ijk}(x,y_*)y^jy^k=\lambda g_{ij}y^j,\quad ||y||_g=a.\qquad (*)$$

b) For $g=\delta$ and $a=1$, (*) leads to the classic eigenvalue problem for C.

c) For $y_*=y$, (*) provides a trivial l.h.s. of the $Z-$spectral equation, with unique $Z-$eigenvalue $\lambda=0$ and $Z-$eigenspace given by:

(i) the scaled proper Finslerian indicatrix (for $a>0$);

(ii) the set of isotropic vectors of the Finsler pseudo-norm (for $a=0$), and

(iii) the negative scaled Lagrangian indicatrix (for $a<0$).

As well, for the metric-extended even-tensor we generally have

Corollary 6.4. *a) For $T\in\Gamma(\widetilde{TM}\times_M T^0_{2k})$ $(k\geq 1)$, the $Z-$spectral equation admits the following invariant extension:*

$$\iota^{2k-1}_{\mathcal{C}}T=\lambda\iota_{\mathcal{C}}g,\quad ||\mathcal{C}||_g=a,\quad a\in\mathbb{R}.$$

b) In the particular case when $T=\tilde{g}\in\Gamma(\widetilde{TM}\times_M T^0_2)$ is a Finslerian metric tensor at the fixed flagpole $(x,y_*)\in M\times T_xM$, for $g=\delta$ and $a=1$, the $Z-$spectral equation from above leads to the classic eigenvalue problem for $\tilde{g}$,

$$\tilde{g}_{ij}y^j=\lambda y^i,\quad ||y||_2=1.$$

We should note that, among the applicative fields of the $Z-$eigendata theory, one can mention: tensor data analysis; higher-order statistics; computer tomography and M.R.I. data processing; multispectral image restoration and compression; signal processing, separation and denoising, etc.

As well, works have been recently addressing open problems, like: the usage of resolvent advances on proper identifying the spectra; optimizing the decomposition for speed and storage data; specializing the spectral algorithms for Big Data within neuro-fuzzy systems for pattern recognition.

References

[1] K. C. Chang, K. Pearson and T. Zhang, On eigenvalue problems of real symmetric tensors, Journal of Mathematical Analysis and Applications 350 (2009), 416-422.

[2] L. Qi, Eigenvalues of a real supersymmetric tensor, Jour. Symb. Comp. 40 (2005), 1302-1324.

[3] A. Cichocki, N. Lee, I. V. Oseledets, A. H. Phan, Q. Zhao and D. P. Mandic, Tensor networks for dimensionality reduction and large-scale optimization: part 1 low-rank tensor decompositions, Found. Trends Mach. Learn. 9 (4-5) (2016), 249-429.

[4] P. Comon, Tensor diagonalization, a useful tool in signal processing, In: IFAC-SYSID, 10th IFAC Symposium on System Identification (Copenhagen, Denmark, July 4-6, 1994. Invited Session), Blanke M., Soderstrom T. (eds), 1 (1994), 77-82.

[5] B. Jiang, S. Ma and S. Zhang, Tensor principal component analysis via convex optimization, Mathematical Programming 150, 2 (2015), 423-457.

[6] L. de Lathauwer, B. de Moor and J. Vandewalle, A multilinear SVD, SIAM J. Matrix Anal. Appl. 21 (2000), 1253-1278.

[7] L. Qi, W. Sun and Y. Wang, Numerical multilinear algebra and its applications, Front. Math. China 2(4) (2007), 501-526.

[8] N. Vannieuwenhoven, N. Vanbaelen, K. Meerbergen and R. Vandebril, The dense multiple-vector tensor-vector product: An initial study, Report TW 635, Katholieke Universiteit Leuven, Department of Computer Science, 2013.

[9] Z. Shen, Differential geometry of spray and Finsler spaces, Springer, 2001.

[10] D. Bao, S-S. Chern and Z. Shen, An introduction to Riemann-Finsler geometry, Springer-Verlag, 2000.

[11] I. Bucataru and R. Miron, Finsler-Lagrange geometry. Applications to dynamical systems, Editura Academiei Romane, Bucuresti, 2007.

[12] X. Cheng and Z. Shen, Finsler Geometry: An Approach via Randers Spaces, Springer, 2013.

[13] R. Miron and M. Anastasiei, Vector bundles. Lagrange spaces. Applications to relativity, Geometry Balkan Press, 1996.

[14] V. Balan, Spectra of multilinear forms associated to notable m-root relativistic models, Linear Algebra and Appl. (LAA), online http://dx.doi.org/10.1016/j.laa.2011.06.033; 436, 1, 1 (2012), 152-162.

[15] V. Balan, Spectral properties and applications of numerical multilinear algebra of $m-$th root structures, Hypercomplex Numbers in Geom. Phys. 2(10), 5 (2008), 101-107.

[16] V. Balan, G. Bogoslovsky, S. Kokarev, D. Pavlov, S. Syparov and N. Voicu, Geometrical models of the locally anisotropic Space-Time, Hypercomplex Numbers in Geom. Phys., Moscow, 1(15), 8 (2011), 4-37.

[17] M. D. Cirillo, R. Mirdell, F. Sjoberg and T. Pham, Tensor decomposition for colour image segmentation of burn wounds, Sci. Rep. 9 (2019), 3291.

[18] Y. Zhang, J. Liu, S. Yang and Z. Guo, Joint image denoising using self-similarity based low-rank approximations, Institute of Computer Science and Technology, Peking University, Beijing 100871, China; 2013 Visual Communications and Image Processing (VCIP).

[19] D. Goldfarb and Z. (Tony) Qin, Robust Low-Rank Tensor Recovery: Models and Algorithms, SIAM J. Matrix Anal. Appl., 35(1) (2019), 225-253.

[20] S. Zhang, X. Guo, X. Xu, L. Li andC-C Chang, A video watermark algorithm based on tensor decomposition, Math Biosci Eng. 16(5) (2019), 3435-3449.

[21] J. Li, J. Bien and M. Wells, HO-SVD package, 2019; https://rdrr.io/github/jamesyili/rTensor/

[22] ____, MATLAB Tensor Toolbox, Version 2.6.

[23] ____, Tensorlab demos, www.tensorlab.net/demos/basic.html, www.tensorlab.net/demos/mlsvd.html.

[24] ____, Sandia Laboratories webpage, https://www.sandia.gov/ tgkolda/TensorToolbox/reg-2.6.html

[25] ____, Tensor Toolbox webpage, https://www.tensortoolbox.org

[26] ____, Htucker webpage (Matlab toolbox for HO-SVD), Czech Republic, https://www.swmath.org/software/9637

[27] V. Balan and N. Perminov, Applications of resultants in the spectral m-root framework, Appl. Sci. (APPS), 12 (2010), 20-29.

[28] V. Balan, H. V. Grushevskaya, N. G. Krylova, M. Neagu and A. Oana, On the Berwald-Lagrange scalar curvature in the structuring process of the LB-monolayer, Applied Sciences 15 (2013), 30-42.

[29] V. Balan, H. V. Grushevskaya and N. G. Krylova, Finsler geometry approach to thermodynamics of first order phase transitions in monolayers, Differential Geometry - Dynamical Systems, 17 (2015), 24-31.

[30] V. Balan and J. Stojanov, Finsler-type estimators for the cancer cell population dynamics, Publications de l'Institut Mathematique, Publisher: Mathematical Institute of the Serbian Academy of Sciences and Arts, Beograd, 98(112) (2015), 53-69.

[31] V. Balan, J. Stojanov, Anisotropic metric models in the Garner oncologic framework, ROMAI J. 10, 1 (2014), 1-10.

[32] L. Astola and L. Florack, Finsler Geometry on higher order tensor fields and applications to High Angular Resolution Diffusion Imaging, International Journal of Computer Vision 5567 (3) (2009), 224-234, DOI:10.1007/978-3-642-02256-2_19.

[33] H. Shimada, On Finsler spaces with the metric $L = \sqrt[n]{a_{i_1 i_2 \dots i_n}(x) y^{i_1} y^{i_2} \dots y^{i_n}}$, Tensor N.S., 33 (1979), 365-372.

[34] P. L. Antonelli, R. S. Ingarden and M. Matsumoto, The theory of sprays and Finsler spaces with applications in physics and biology, Kluwer Academic Publishers, Fundamental Theories of Physics 58, Netherlands, 1993.

Please cite this article using:

Vladimir Balan, On spectral data and tensor decompositions in Finslerian framework, AUT J. Math. Comput., 2(2) (2021) 153-163
DOI: 10.22060/ajmc.2021.20213.1059